Applied Nanoscience (2021) 11:301–308
https://doi.org/10.1007/s13204-020-01588-4

ORIGINAL ARTICLE

Controllable fabrication and magnetic properties of Nd/Co core/shell nanowires

Hongyan Li[1] · Yunze Long[2] · Xiaoxiong Wang[2] · Guojun Song[1] · Lichun Ma[1] · Hui Xu[1] · Xiaoru Li[1]

Received: 1 September 2020 / Accepted: 13 October 2020 / Published online: 28 October 2020

Abstract

Ordered Nd/Co_{100} and Nd/Co_{200} core/shell nanowire arrays with lengths of ~ 10 μm and diameters of 100 nm and 200 nm were fabricated by two-step electrodeposition into anodic alumina oxide templates. Co-*hcp* phases were observed in the Nd/Co_{100} and Nd/Co_{200} nanowires. Hysteresis curves obtained from the Nd/Co_{100} and Nd/Co_{200} nanowires showed that the squareness ratio of the parallel nanowire long axis was greater than that of the perpendicular nanowire long axis. The magnetic properties indicated that the easy axis was parallel to the long axis. The coercivity and parallel squareness ratio in the Nd/Co_{200} nanowires were greater than those in the Nd/Co_{100} nanowires, which demonstrated that the Nd/Co_{200} nanowires exhibited hard magnetism behavior.

Keywords Core/shell nanowires · AAO template · Magnetocrystalline anisotropy · Shape anisotropy · Magnetostatics interaction

Introduction

Magnetic nanowires, including multilayered, alloyed and core/shell composite nanowires, have attracted much interest in recent years due to their attractive fundamental properties, multifunctionality and wide range of potential applications (Salgueiriño-Maceira and Correa-Duarte 2007; Kim et al. 2005). The dipolar interaction is difficult to investigate scientifically due to its long-range nature, which depends sensitively upon the arrangement of the magnetic entities (Wang et al. 2019). Magnetic core/shell nanowires make it possible to fix the geometric parameters to investigate the complex magnetic interaction, and have become increasingly favored over uniform nanoscale materials due to their emerging novel and exotic properties (Mejia-Lopez et al. 2019). Technologically, the magnetic parameters can be tuned by modifying the core or shell composition and geometric parameters to meet the requirements of various applications. Materials which form nanotubes can be used as shells, whether magnetic or non-magnetic, e.g. polymers (Li et al. 2016), carbon (Jiao et al. 1996), ferromagnetic metals (Li et al. 2010), and metal oxides (Ali et al. 2016). Core materials can also be magnetic or non-magnetic. In numerous experiments, researchers have broadly examined the dependence of the core/shell nanowires upon factors, such as fabrication procedure, crystal structure, size, shape, and composition. Core/shell nanowires are characterized by the combination of properties of each kind of materials; hence, these provide the geometric parameters for investigating the complex interactions.

Various methods have been reported for the synthesis of core/shell nanowires, including wet chemical vapor deposition (CVD) (Kim et al. 2010), gas-phase (Sumiyama et al. 2005), vapor deposition (Gautam et al. 2008), the sol-gel method (Son et al. 2006), the hydrothermal synthesis method (Zhang and Zeng 2010) and the two-step electrodeposition process (Li et al. 2014). Among these, the template-assisted electrodeposition method has become a widespread and useful synthesis strategy due to its ordered honeycomb structure, pore diameter, the distance between pores and membrane thickness (Masuda and Fukuda 1995; Huang et al. 2013; Gong et al. 2008). As well as affording easy control

✉ Xiaoru Li
lixiaoruqdu@126.com

1 Institute of Polymer Materials, School of Material Science and Engineering, Qingdao University, No. 308 Ningxia Road, Qingdao 266071, Shandong, People's Republic of China

2 School of Physical Sciences, Qingdao University, No. 308 Ningxia Road, Qingdao 266071, Shandong, People's Republic of China

of the required compound composition, this approach is economical and easy to perform. The magnetic properties of core/shell nanowires have been found to be related to the dimensions and spatial arrangements (relative lengths, diameters) (Kalska-Szostkoa et al. 2019), chemical elements, construction, shape anisotropy, magnetostatic interaction, and magnetocrystalline anisotropy. Although films of La–Co (Yuan and Liu 2006) and La–Ni–Co (Tan et al. 2006) have been successfully prepared using DC electrodeposition, the preparation of rare-earth (RE)/ferromagnetic metal (FM) core/shell nanowires has been rarely reported. In our previous work, the fabrication of the RE/FM/polymer nanocables was reported (Li et al. 2018, 2020), we have found the coercive force and the squareness with the applied field parallel to the axis of the nanocables increased dramatically compared with the FM nanotubes. Neodymium (Nd) and ferromagnetic metals have, therefore, been selected for the preparation of core/shell nanowires, an idea inspired by permanent magnets composed of ferromagnetic metals and RE metals. Such RE/ferromagnetic material nanowires are expected to have outstanding magnetic and optical properties. The aim of the present work is to develop novel multifunctional nanomaterials based on the physical properties related to microstructure and composition. The idea that two-dimensional magnetic films can be used to make sensors (Liu et al. 2019) gave us some insight into the future of using these ordered arrays of magnetic nanowires to make two-dimensional films for assembling nanoscale devices.

The controllable assembly of Nd/Co core/shell nanowires with various sizes in anodic aluminum oxide (AAO) templates by a two-step DC electrodeposition method is reported in the present work. The Co nanotube shell was first obtained in the AAO template and the Co/AAO then served as a second template for the deposition of Nd. Co was selected to be used as the shell because the Co nanoparticle grows from bottom to top and tends to form nanotubes, while the Nd core tends to form nanowires.

Experimental

Fabrication

The Nd/Co core/shell nanowire arrays on AAO templates were obtained according to the following methods and conditions. Anodic aluminum oxide (AAO) templates with thicknesses of ~ 60 μm and diameters of 0.2 μm and 0.1 μm were purchased from Whatman Ltd. The AAO templates were immersed in ethanol for ultrasonic washing (10 s). After volatilization of the ethanol, a gold (Au) layer was sputtered onto one side of the AAO template as the working electrode. With a sufficiently long sputtering time, the Au nanolayer sealed the pores on the bottom of the AAO template, thus allowing the growth of nanowires. In the three-electrode cell, a platinum plate was used as a counter electrode and a saturated calomel electrode was used as the reference electrode. The Co^{2+} electrolytic solution containing 0.5 M $CoSO_4{\cdot}7H_2O$ (Co^{2+} is 0.5 M), 0.2 M H_3BO_3 and 0.2 M KCl was prepared by dissolving reagent-grade chemicals in deionized water. The pH of the mixture was in the range of 4.0–4.5. The Co^{2+} was reduced on the electrochemical analyzer (Chi 730) at a constant DC voltage amplitude of -0.9 V with stirring. The Co nanotubes were obtained with a growth time of 18 min. The Co/AAO membrane was then used as a secondary template for the deposition of Nd from a mixed solution of 0.2 M $Nd(NO_3)_3{\cdot}nH_2O$ (Nd^{3+} is 0.2 M), 0.2 M H_3BO_3 and 0.2 M KCl. The pH of the mixture was controlled in the range of 5.0–5.5, the DC voltage was set to − 3.0 V, and the growth time was 50 min. The samples prepared using the 100 nm and 200 nm diameter AAO templates were accordingly labeled Co_{100}, Co_{200}, Nd/Co_{100}, and Nd/Co_{200}.

The preparation of Nd/Co core/shell nanowire arrays is shown schematically in Fig. 1. The SEM images of the top and lateral views of AAO are presented in Fig. 1a and b.

Characterization

JEOL JSM-6390LV scanning electron microscope (SEM) was used to characterize the morphology of samples. Philips CM200-FEG transmission electron microscope (TEM) was carried to obtain TEM images. The crystal structures were determined by selected-area electron diffraction (SAED) pattern. For SEM measurement, Nd/Co/AAO was immersed in 3 M NaOH solution for 2 h to remove the AAO template, and then the sample was washed with deionized water and ethanol, respectively. For TEM measurement, Nd/Co nanowires were dispersed in ethanol, a drop of diluted sample was placed on a copper grid and evaporated prior to observation. The elemental composition of nanowires was detected by X-ray diffraction (XRD) at a rate of 2° per min over a diffraction range of 10° to 80°and energy-dispersive X-ray spectroscopy (EDS), respectively. Magnetic properties, coercive field, and residual magnetism of the sample were tested by Physical Property Measurement System (Quantum Design-PPMS).

Results and discussion

The SEM images of Co_{100} and Co_{200} nanotubes after removal of the AAO templates were presented in Fig. 2a and b, respectively. The nanotubes were clearly seen to be homogeneous and open at the top. The tubular structure was verified by the TEM images (Fig. 2c and d), where the Co_{100} and Co_{200} nanotubes were seen to be hollow with a

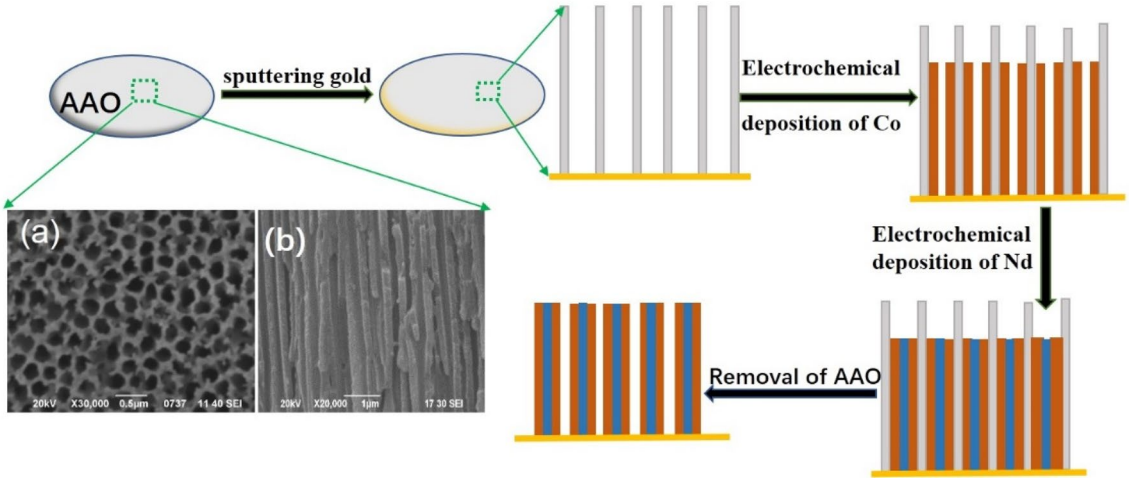

Fig. 1 Schematic illustration for the preparation process, SEM of AAO template **a** top view, **b** sectional view

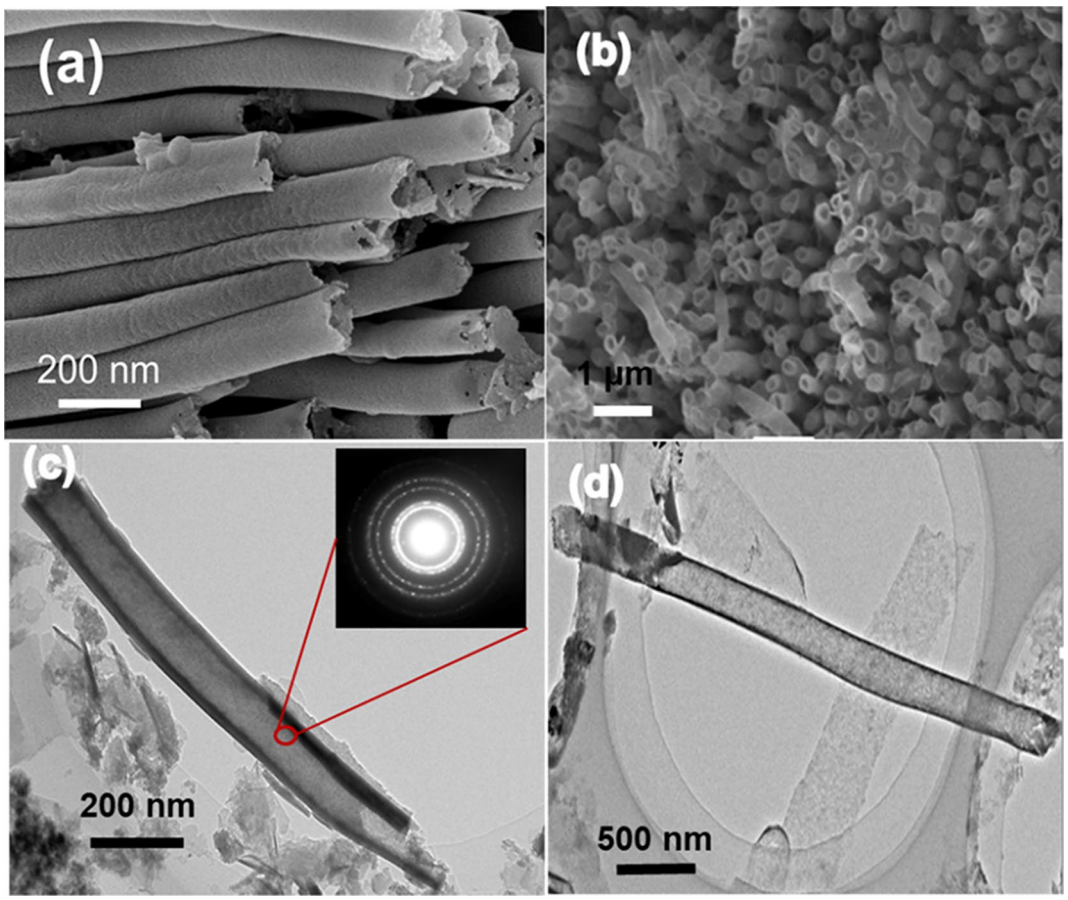

Fig. 2 SEM images of **a** Co_{100}, **b** Co_{200}, TEM images of **c** Co_{100}, **d** Co_{200}. The inset of (**c**) is SAED pattern of Co nanotubes

continuous wall. The wall thickness of the nanotubes was approximately 20 nm. Selected area electron diffraction (SAED) revealed that the Co nanotube was polycrystalline (Sumiyama et al. 2005).

The morphology of the Nd/Co core/shell nanowire arrays was indicated by the SEM and TEM images in Fig. 3. In Fig. 3a, the Nd/Co_{100} nanowire arrays (~ 12 μm length) were seen to be neatly arranged and parallel to each other.

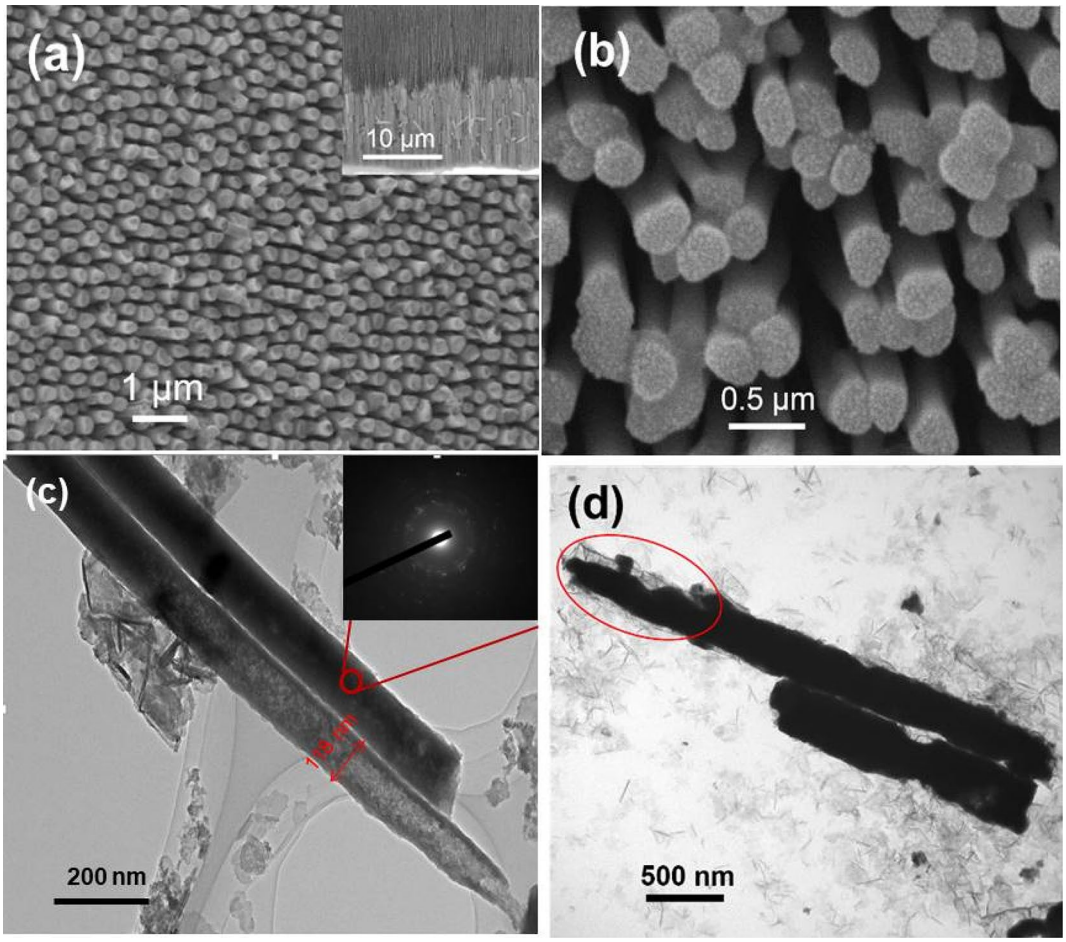

Fig. 3 SEM images of **a** Nd/Co_{100}, **b** Nd/Co_{200}. The inset of **a** is SEM image of longitudinal profile, TEM images of **c** Nd/Co_{100}, **d** Nd/Co_{200}. The inset of (**c**) is SAED pattern of Nd/Co nanowires

Figure 3b indicated that the Nd/Co_{200} nanowires were solid, uniform and highly dense. Figure 3c showed that the Nd core filled the Co nanotubes, with a clear contrast between Co shell and Nd core. The diameter of the Nd/Co nanowire was about 118 nm. Filling traces could also be seen at the ends (red marks, Fig. 3d) due to the fact that a small number of Nd atoms had not yet properly aligned at the end of deposition.

Typical SEM images of the Nd/Co_{100} nanowires and corresponding element mapping images were shown in Fig. 4. Figure 4a and b were typical SEM images with different magnification. Elemental mapping images (Fig. 4c and d) from Fig. 4b demonstrated the existence of Co and Nd elements with uniform distribution, thus confirming the successful generation of the Nd/Co_{100} nanowires.

The chemical composition of the Nd/Co_{100} nanowires was examined by energy-dispersive X-ray spectroscopy (EDS), as presented in Fig. 5a. These results confirmed the presence of Co and Nd along with other elements, such as Cu, O, Al and Au. The peaks corresponding to Cu and Al likely caused sample stage and incomplete etching, the peaks corresponding to Au were likely caused by sputtering before SEM measurement, and O may be derived from oxidation of the metals. The XRD patterns of the Nd/Co nanowire arrays obtained while they were embedded in the AAO templates are presented in Fig. 5b. The XRD patterns of the Nd/Co_{100} and Nd/Co_{200} nanowires were the same. The formation of polycrystalline Co-*hcp* revealed a texture along the (100, (002)) and (110) directions, which was observed for all the samples. This would have a strong influence upon magnetocrystalline anisotropy. Bragg peaks appeared at $2\theta = 41.6°$, 44.7°, and 75.9°, corresponding to Co (100)-*hcp*, Co (002)-*hcp* and Co (110)-*hcp*, respectively. However, there were no diffraction peaks from Nd. It was speculated that the high deposition rate (the deposition voltage was − 3.0 V) leads to the failure of neodymium crystal phase. Notably, the XRD pattern also shows four strong peaks close to $2\theta = 38°$, 44.4°, 64.5°, and 77.6° which are assigned to Au-*fcc* (111), (200), (220) and (311) sputtered on the back side of the AAO template.

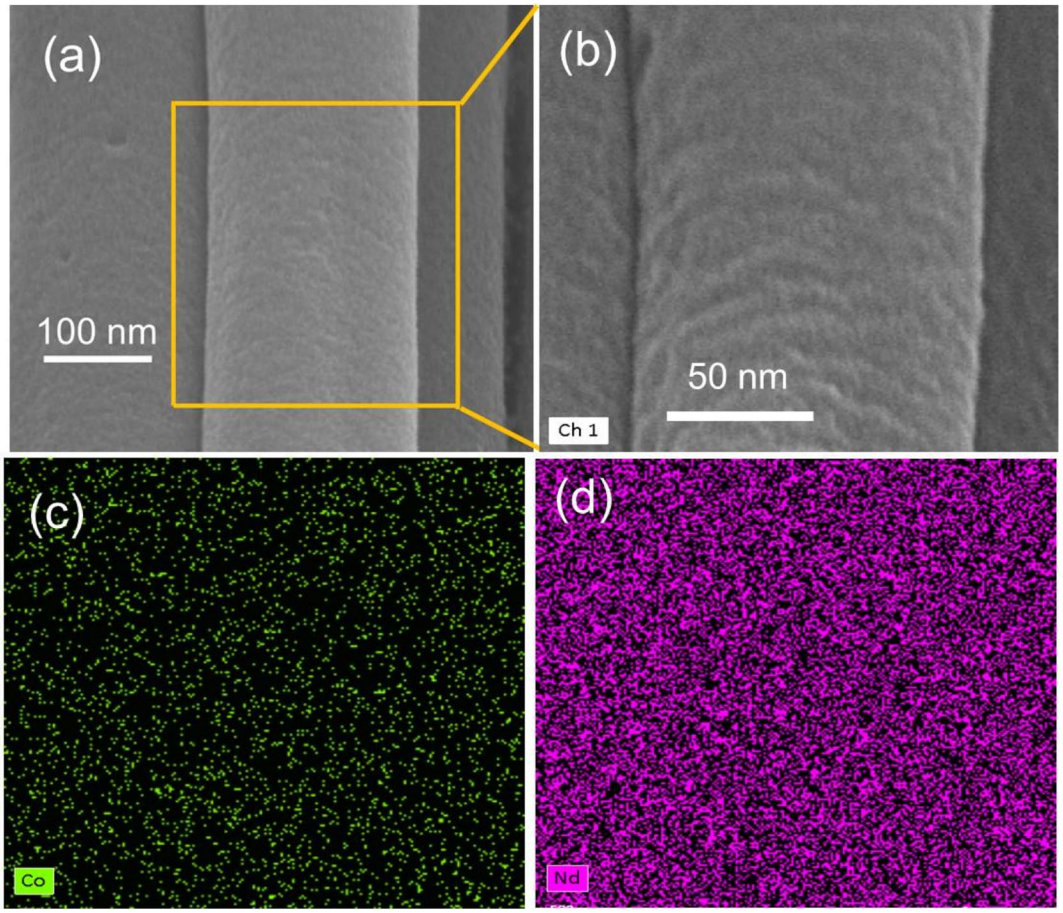

Fig. 4 SEM images of Nd/Co_{100} (**a**) and (**b**), (**c**) and (**d**) the elemental mapping images for Co and Nd elements

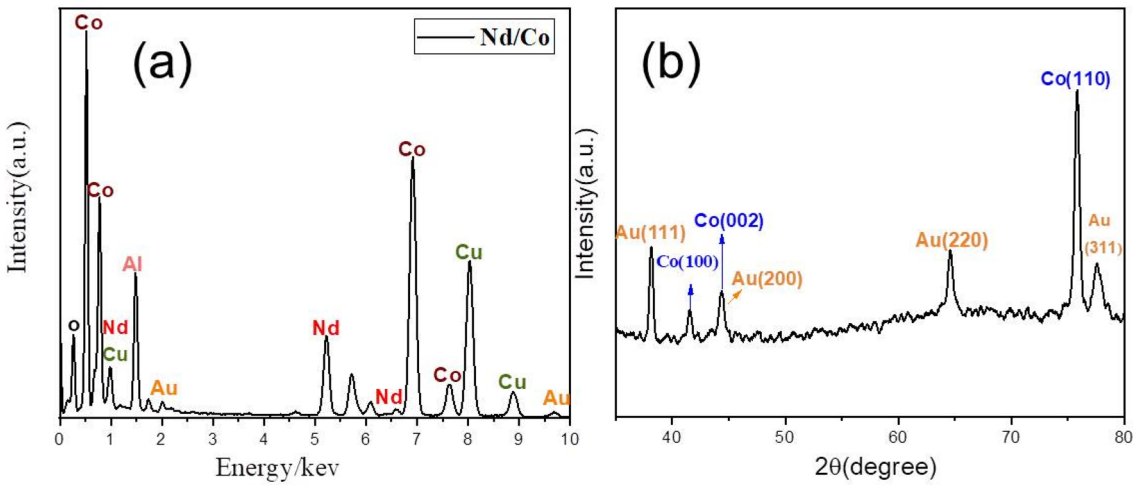

Fig. 5 **a** EDX spectra and **b** XRD patterns of Nd/Co nanowires

The magnetic properties of the Co nanotube arrays and Nd/Co core/shell nanowire arrays embedded in the AAO templates were characterized by at 298 K. The magnetic hysteresis (M-H) loops for all samples were presented in Fig. 6 with applied magnetic field both parallel to the nanotube/nanowire axis and perpendicular to the nanotube/

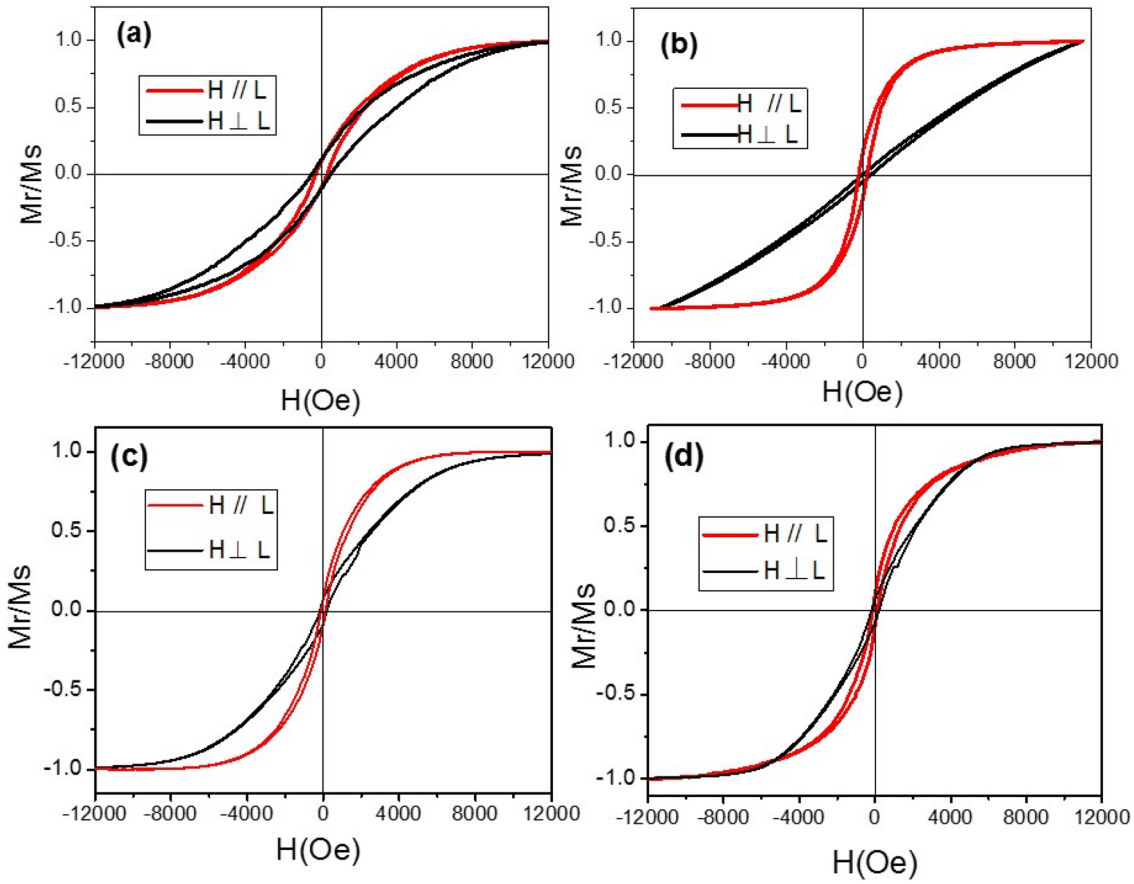

Fig. 6 H-M loops of **a** Co_{100} nanotubes, **b** Co_{200} nanotubes, **c** Nd/Co_{100} nanowires, **d** Nd/Co_{200}nanowires, the "//" and "⊥" indicate the applied field is parallel to and perpendicular to the long axis, respectively

Table 1 Magnetic parameters of Co nanotubes and Nd/Co nanowires

Sample	$H_c^{//}(Oe)$	$H_c^{\perp}(Oe)$	$SQ^{//}$	$SQ^{\perp}$
Co_{100} NTs	310	498	0.110	0.098
Co_{200} NTs	220	234	0.170	0.031
Nd/Co_{100} NWs	123.0	177.0	0.083	0.081
Nd/Co_{200} NWs	147.4	203.3	0.121	0.062

nanowire axis. The M-H loops in Fig. 6a and b indicated that the Co_{100} nanotube arrays had greater coercivity ($Hc^{//}=310$ *Oe*, $Hc^{\perp}=498$ *Oe*) than the Co_{200} ($Hc^{//}=220$ *Oe*, $Hc^{\perp}=234$ *Oe*) nanotubes, which could be attributed to small grain size. The magnetic properties of all the samples were indicated in Table 1. However, the value of parallel squareness ratio ($SQ^{\parallel}$) was a little greater than that of perpendicular squareness ($SQ^{\perp}$). According to the literature (Xu et al. 2016), the shape anisotropy tends to induce magnetization orientation parallel to the long axis, while the magnetostatic interaction makes the easy axis perpendicular to the long axis. Hence, the shape anisotropy predominated over the magnetostatics interaction in the Co nanotubes. For the Nd/Co_{100} nanowire arrays (Fig. 6c), the values of *Hc* ($Hc^{//}=123$ *Oe*, $Hc^{\perp}=177$ *Oe*) and *SQ* ($SQ^{//}=0.081$, $SQ^{\perp}=0.083$) were lower than those of the Co_{100} nanotube arrays, and the $SQ^{\parallel}$ and $SQ^{\perp}$ were nearly the same. This may indicate an increased magnetostatic interaction due to the existence of the Nd nanowires, which reduced *Hc* and *SQ* of the Nd/Co_{100} nanowires. The influence of the magnetostatic interaction had a similar effect for the Nd/Co_{200} nanowires, reducing the *Hc* and *SQ* of the Nd/Co_{200} nanowires compared to the Co_{200} nanotubes. However, the value of $SQ^{\parallel}$ was greater than that of $SQ^{\perp}$ for both Nd/Co_{100} and Nd/Co_{200} nanowires. This clearly indicated that the easy magnetization axis was parallel to the long axis. The coercivity ($Hc^{//}=147.4$ *Oe*, $Hc^{\perp}=203.3$ *Oe*) and $SQ^{\parallel}$ (0.121) in the Nd/Co_{200} nanowires were greater than those in the Nd/Co_{100} nanowires. In particular, the saturation magnetization of the Nd/Co_{200} nanowires was one order of magnitude larger than that of the Nd/Co_{100} nanowires, which indicated that the Nd/Co_{200} nanowires exhibit hard behavior.

The magnetocrystalline anisotropy was another factor affecting the anisotropy field of nanowires (Wang et al. 2010; Shamaila et al. 2009; Han et al. 2003). The easy axis was parallel to the wire axis due to the presence of *hcp*-Co.

It was notable that the prepared Nd/Co nanowire arrays had greater *SQ* than those of Co–Ni core/shell nanowires (Wang et al. 2019), and Co/BCO core/shell nanowires (Khan et al. 2016). The magnetic storage also depended on the values of coercivity and residual magnetization ratio at a large level (Huh et al. 2014; Adam 1966). So, the Nd/Co nanowires are expected to have a wide range of applications.

Conclusion

In summary, novel magnetic Nd/Co core/shell nanowire arrays were successfully prepared in AAO templates with same lengths of ~ 10 μm and different diameters via a two-step electrodeposition process at room temperature. The hysteresis loops of the Nd/Co nanowire arrays indicated clear magnetic anisotropy, with the easy axis parallel to the long axis, which was induced by the shape anisotropy. The Nd/Co_{200} nanowires displayed larger values of *Hc* and $SQ^{//}$ than those of Nd/Co_{100} nanowires and other core/shell nanowires. Although the magnetostatic interaction reduced the coercivity and squareness ratio of Nd/Co nanowires, the coercivity and squareness ratio of the Nd/Co nanowires prepared in this work were still greater than those of cobalt-based nanowires with similar structures. Therefore, the prepared Nd/Co core/shell nanowires are expected to have a wide range of applications.

Acknowledgements This work was supported by the project of Natural Science Foundation of China, China (NO. 51903129), China postdoctoral Science Foundation, China (No. 2017M612196, No. 2017M612197), Shandong Province Natural Science Fund of China (No. 2014ZRB01840), and Qingdao Postdoctoral Scientific Research Foundation.

Compliance with ethical standards

Conflict of interest The authors declare that they have no conflict of interest.

References

Adam GD (1966) Physical principles of magnetism. Nature 210:451–452

Ali SS, Li WJ, Javed K, Shi DW, Riaz S, Zhai GJ, Han XF (2016) Exchange bias in two-step artificially grown one-dimensional hybrid Co-$BiFeO_3$ core-shell nanostructures. Nanotechnology 27:045708

Gautam UK, Fang XS, Bando Y, Zhan J, Golberg D (2008) Synthesis, structure, and multiply enhanced field-emission properties of branched ZnS nanotube-in nanowire core-shell heterostructures. ACS Nano 5:1015–1021

Gong XZ, Tang JN, Li JQ, Liang YK (2008) Preparation and characterization of La-Co Alloy nanowire arrays by electrodeposition in AAO template under nonaqueous system. T Nonferr Metal Soc 18:642–647

Han GC, Zong BY, Luo P, Wu YH (2003) Angular dependence of the coercivity and remanence of ferromagnetic nanowire arrays. J Appl Phys 93:9202–9207

Huang ZL, Meng GW, Huang Q, Chen B, Zhu CH, Zhuo Z (2013) Large-area Ag nanorod array substrates for SERS: AAO template-assisted fabrication, functionalization, and application in detection PCBs. J Raman Spectrosc 44:240–246

Huh SH, Gang HL, Chang Y (2014) Potential perpendicular magnetic recording material: supported and unsupported vertically-grown ferromagnetic iron nanowire arrays. J Korean Phys Soc 65:717–721

Jiao J, Seraphin S, Wang X, Withers J (1996) Preparation and properties of ferromagnetic carbon-coated Fe Co, and Ni nanoparticles. J Appl Phys 80:103–108

Kalska-Szostkoa B, Klekotkaa U, Olszewskib W, Satuła D (2019) Multilayered and alloyed Fe-Co and Fe-Ni nanowires physicochemical studies. J Magn Magn Mater 484:67–73

Khan U, Irfan M, Li WJ, Adeel N, Liu P, Zhang QT, Han XF (2016) Diameter-dependent multiferroic functionality in hybrid core/shell NWs. Nanoscale 8:14956–14964

Kim H, Achermann M, Balet LP, Hollingsworth JA, Klimov VI (2005) Synthesis and haracterization of Co/CdSe core/shell nanocomposites: bifunctional magnetic-optical nanocrystals. J Am Chem Soc 127:544–546

Kim HE, Kim HS, Na HG, Yang JC, Lee C (2010) Preparation and annealing of GaN/Cu Core-shell nanowires. J Alloys Compd 2:175–180

Li XR, Wang YQ, Song GJ, Peng Z, Yu YM, She XL, Sun J, Li JJ, Li PD, Wang ZF, Duan XF (2010) Fabrication and magnetic properties of Ni/Cu Shell/Core nanocable arrays. J Phys Chem C 15:6914–6916

Li XR, Li PD, Song GJ, Peng Z, Feng SY, Zhou CJ (2014) Synthesis and magnetic properties of Ni/Fe shell/core nanocable arrays. Mater Lett 122:58–61

Li XR, Yang C, Han P, Zhao QP, Song GJ (2016) Facile synthesis and magnetic study of Ni@polyamide 66 coaxial nanotube arrays. J Magn Magn Mater 419:57–61

Li XR, Wang XX, Ma LC, Peng Z, Yang C, Han P, Li HY, Miao YC, Long YZ, Song GJ (2018) Effect of each layer on anisotropic magnetic properties of Nd/Fe/polyamide 66 three-layer coaxial nanocables. ACS Omega 3:3617–3621

Li HY, Song GJ, Ma LC, Xu H, Sun SY, Shi JR, An MR, Li XR (2020) Structural, magnetic, and fluorescence properties of Nd/Ni/PA66 multilayer coaxial nanocables. Physica E 117:113824

Liu Y, Zhang S, He J, Wang ZM, Liu Z (2019) Recent progress in the fabrication, properties, and devices of heterostructures based on 2D materials. Nano-Micro Lett 11:13

Masuda H, Fukuda K (1995) Ordered Metal nanohole arrays made by a two-step replication of honeycomb structures of anodic alumina. Science 268:1466–1468

Mejia-Lopez J, Tangarife E, Mazo-Zuluaga J (2019) Physical-chemical properties of M@Fe_3O_4 Core@Shell Nanowires (M=Cu Co, CoO). Phys Chem Chem Phys 21:4584–4593

Salgueiriño-Maceira V, Correa-Duarte MA (2007) Increasing the complexity of magnetic core/shell structured nanocomposites for biological applications. Adv Mater 19:4131–4144

Shamaila S, Liu DP, Sharif R, Chen JY, Liu HR, Han XF (2009) Electrochemical fabrication and magnetization properties of CoCrPt nanowires and nanotubes. Appl Phys Lett 94:212502

Son SJ, Bai X, Nan A, Ghandehari H, Lee SB (2006) Template synthesis of multifunctional nanotubes for controlled release. J Controlled Release 114:143–152

Sumiyama K, Hihara T, Peng D, Katoh R (2005) Structure and magnetic properties of Co/CoO and Co/Si core-shell cluster assemblies prepared via gas-phase. Sci Technol Adv Mat 6:18–26

Tan SZ, Yuan DS, Liu YL (2006) Study on the pulse electrodeposition of La-Ni-Co alloy from dimethylsulfoxide. Mater Lett 16:2055–2058

Wang ZX, Teng QY, Dai XG, Huang HB, Zhang SM, Zhang X, Xu DW, Li PF, Li ZJ (2010) Development of influenza virus PR8 mutants and their characteristics on embryonated chicken eggs. Vet Sci China 40:788–792

Wang J, Xiong W, Huang L, Li YX, Zuo ZL, Hu XY, Wang T, Xiao JQ, Hu J (2019) Electrochemical synthesis of core-shell Co-Ni nanorod arrays with facilely regulated magnetic properties. Phys B 567:113–117

Xu Q, Wang ZJ, Wang YG, Sun HY (2016) The effect of Co content on the structure and the magnetic properties of Co_xNi_{1-x} nanotubes. J Magn Magn Mater 419:166–170

Yuan DS, Liu YL (2006) Electrochemical preparation La-Co magnetic alloy films from dimethylsulfoxide. Mater Chem Phys 1:79–83

Zhang S, Zeng HC (2010) Solution-based epitaxial growth of magnetically responsive Cu@Ni nanowires. Chem Mater 4:1282–1284